

## CHAPTER IV

### THE CRYSTALLINE PHASE OF POLYVINYLIDENE FLUORIDE FILM

#### 4.1 Abstract

Poly vinylidene fluoride (PVDF) is a semi-crystalline polymer which shows polymorphism and is commonly crystallized in non-polar crystalline  $\alpha$  phase. It has found various applications during the last decades and the most important applications lies in its pyro- piezoelectric properties. The  $\beta$  phase content is of prime importance in these applications so that the increasing of  $\beta$  phase content in PVDF has been concern in this field. In this study, the fabrication of PVDF film is divided to two methods. The solution casting and compression molding were employed in this research. The effect of drawn compression film and solution-crystallized PVDF in DMF were studied through the specific FTIR absorption bands of  $\alpha$  and  $\beta$  phases. FTIR is a well known technique for detecting changes in the content of  $\beta$  phase in both solution cast and compression. SEM reveals surface micrograph of films produced from solution casting and compression. Many voids from evaporating solvent can be observed on the surface of solution casting film. From these results, compressed PVDF film seems more practical to be employed in this research. The  $\beta$  phase of compressed films is confirmed by X-ray diffraction (WAXD). The dielectric constant and dielectric loss tangent of compressed PVDF at different draw ratio are investigated showing the enhancement of dielectric constant when the draw ratio increases. From  $d_{33}$  meter shows the draw ratio of compressed PVDF film has significantly affected to the piezoelectric coefficient. The more content of  $\beta$  crystalline phase in compressed PVDF film enhances the piezoelectric coefficient. The melting temperature has not been affected by mechanical drawing of the film. Dramatically changed in crystallinity with draw ratio is observed.

## 4.2 Introduction

Poly vinylidene fluoride (PVDF) can be easily processed and has excellent mechanical properties, high chemical resistance and good thermal properties as well as high pyro- and piezoelectric coefficient [Mohammadi, B., *et al.* 2007]. Therefore, PVDF have been exploited in the improvement of electronic devices. Besides its pyro- and piezoelectric properties, which are of great technological importance, PVDF displays a well-known polymorphism depending on crystallization conditions. Many investigations have been carried out to characterize PVDF crystalline structure as directs results with electric properties. Many crystals phases have been reported for this polymer [Mohammadi, B., *et al.* 2007][ Rollik, D., *et al.* (1999)]. However two crystals which have recently attracted much interest for their pyro-and piezoelectric are  $\alpha$  phase and  $\beta$  phase [Ye, Y., *et al.* 2004]. In the  $\alpha$  phase, chain is in a sequence of alternating trans and gauche sequences, resulting in no net dipole. In the  $\beta$  phase, chains are in an all-trans planar zigzag conformation, resulting in a significant dipole moment lateral to the chain axis. Therefore,  $\beta$  which owns phase highest pyro- and piezoelectric is exploited in piezoelectric application. This phase can be obtained by mechanical stretching at a given temperature of  $\alpha$  phase as the most importance technique. Higher stretching temperatures reduces the phase conversion efficiency and conversion in to  $\beta$  phases takes place only for stretch ratio above 5 [Salimi, A., *et al.* (2003)].

FTIR spectra of two major phase ( $\alpha$  and  $\beta$  phases) of PVDF have been investigated extensively [Salimi, A., *et al.* (2003)][ Mohammadi, B., *et al.* (2007)][ Kim, B. S., *et al.* (1998)]. Vibrational bands at  $530\text{ cm}^{-1}$  ( $\text{CF}_2$  bending),  $615$  and  $763\text{ cm}^{-1}$  ( $\text{CF}_2$  bending and skeletal bending) and  $795\text{ cm}^{-1}$  ( $\text{CH}_2$  rocking) refer to  $\alpha$  phase. Vibrational bands at  $509\text{ cm}^{-1}$  ( $\text{CF}_2$  bending), and  $840\text{ cm}^{-1}$  ( $\text{CH}_2$  rocking) correspond to  $\beta$  phase [ Mohammadi, B., *et al.* (2007)]. B. Mohammadi, *et al.*, (2007) measured the degree of  $\alpha$  and  $\beta$  crystalline phase, assuming the IR absorption follows Beers 's law. The  $\alpha$ -phase had a  $763\text{ cm}^{-1}$  as characteristic infrared absorption. The  $\beta$  phase had a  $840\text{ cm}^{-1}$  as characteristic infrared absorption.

In this paper, the crystalline structure at different draw ratio is investigated on the  $\beta$  content as well as orientation of the polar  $\beta$  phase which occurs after poling. The influences on dielectric, dielectric loss tangent and  $d_{33}$  as piezoelectric properties are also investigated.

### 4.3 Experimental

#### 4.3.1 Material and film preparation

Poly (vinylidene fluoride) powder manufactured from Solvay Company (Belgium) (Solef 1008) was used. Two methods were utilized to fabricate PVDF thin film. First was solution casting which PVDF powder was dissolved in DMF solution. The viscous solution is then cast on glass substrate. After the solvent evaporation in a stove at 60 °C for 20 minutes under vacuum the sample films of 50-100  $\mu\text{m}$  thickness were obtained. Another method was compression molding which PVDF films were prepared by Wabash compression. From this method, PVDF powder was compressed at 174 °C for 20 minutes under pressure 15 tons. The thickness of the prepared films ranged 100-200  $\mu\text{m}$ . Film produced from compression molding was stretched by stretching instrument to obtain film at different ratio at constant stretching rate of 5 mm/min.

#### 2.2 Instrumental techniques

Infrared spectra were achieved using a FTIR spectrophotometer (Bruker model Vector 3.0) in the wave number range of 400-1000  $\text{cm}^{-1}$ . According to test methods reported in [Salimi, A., *et al.* 2003] the vibration bands at 763 ( $\text{CF}_2$  bending and skeletal bending), correspond to  $\alpha$  phase; whereas vibration band at 840  $\text{cm}^{-1}$  ( $\text{CH}_2$  rocking) is assigned to  $\beta$  phase. The fraction of the  $\beta$  phase was determined by comparing the absorbance of vibration band peaks of the samples at 840  $\text{cm}^{-1}$  and 763  $\text{cm}^{-1}$ . Supposing that IR absorption follows the Lambert–Beer law, the A absorbance is given by  $A = \log(I^0/I) = KCXL$ ; where the thickness of samples is L and

average total monomer concentration is  $C$ ;  $I_0$  and  $I$  are the incident and transmitted intensity radiations, respectively;  $K$  is the absorption coefficient at the respective wave number and  $X$  is the degree of crystallinity of each phase. From the average crystalline densities of  $\alpha$  ( $1.925 \text{ g/cm}^3$ ) and  $\beta$  ( $1.973 \text{ g/cm}^3$ ) phases, a  $C$  value of  $0.035 \text{ mol/cm}^3$  was determined. The absorption coefficients of  $K_\alpha = 6.1 \times 10^4$  and  $K_\beta = 7.7 \times 10^4 \text{ cm}^2/\text{mol}$  at  $763 \text{ cm}^{-1}$  and  $840 \text{ cm}^{-1}$ , feature of  $\alpha$  and  $\beta$  phases, the fraction of  $\beta$  phase,  $F(\beta)$ , can be calculated using the following equation:

$$F(\beta) = \frac{X_\beta}{X_\alpha + X_\beta} = \frac{A_\beta}{(K_\beta + K_\alpha)A_\alpha + A_\beta} = \frac{A_\beta}{1.26 A_\alpha + A_\beta} \quad (1)$$

where  $X_\alpha$  and  $X_\beta$  used in Eq. (1) are crystalline mass fraction of  $\alpha$  and  $\beta$  phases and the  $A_\alpha$  and  $A_\beta$  correspond to absorption bands at  $763$  and  $840 \text{ cm}^{-1}$ , respectively. This equation was used to quantify the FTIR results. In fact, Eq. (1) was used to measure the transformation efficiency of gauche state to trans state in PVDF films [Mohammadi, B., *et al.* 2007]. The micro structure of film which was produced from solution casting and compression molding was observed by scanning electron microscope. A crystal phase of undrawn and drawn PVDF were analyzed by X-ray diffraction (Rigaku, model Dmax 2002) with  $2\theta$  angle ranging from  $5$  to  $90^\circ$  was measured. The reflections corresponding to the  $\beta$  form were analyzed. Undrawn and drawn PVDF film were poled in oil bath polarization process under an electric field of  $100 \text{ kV/mm}$  at  $90^\circ \text{ C}$  (poling time in this temperature was set at  $30 \text{ min}$ ). Stress piezoelectric coefficients ( $d_{33}$ ) of the polarized films were obtained from  $d_{33}$  meter (APC Int. Ltd., model 8000) operating at frequency of  $1000 \text{ Hz}$  and a time interval of  $24 \text{ h}$  after film polarization.

## 4.4 Results and Discussion

### 4.4.1 Phase Characterization

The important advantage of FTIR over other physical characterization techniques is its ability to selectively measure localized conformation, packing, and relative orientation changes. The vibrational spectra of the two principal phases have been analyzed extensively. The characteristic infrared bands of the  $\beta$  crystalline phase for PVDF are  $839\text{ cm}^{-1}$  and those of the  $\alpha$  crystalline phase are  $763$  and  $976\text{ cm}^{-1}$  [Kim, B. S., *et al.* 1998]. The complete predominated for  $\beta$  crystalline phase is found in drawn sample and DMF solution-crystallized PVDF while the predominated phase in undrawn sample is  $\alpha$  crystalline phase. According to Figure 4.1, as draw ratio increases the intensity of the characteristic of the  $\alpha$  crystalline phase decreases whereas the characteristic of the  $\beta$  crystalline phase increases. Even at stretch ratio of 2, the bands at  $763\text{ cm}^{-1}$  are still observable, indicating that  $\alpha$  crystalline phase still remains in the sample. For the DMF solution-crystallized PVDF, polar solvent can reduce the energy required to form a polar crystal ( $\beta$  crystalline phase) but there is no effect on a nonpolar crystal ( $\alpha$  crystalline phase) according to Salami [Salimi, A., *et al.* 2004]. Absorption bands which show in Figure 4.1 are used to calculate the changes in the  $\beta$  crystalline phase in any PVDF film. Appearance of absorption band at  $763$  and  $840\text{ cm}^{-1}$ , feature of  $\alpha$  and  $\beta$  crystalline phases, which is used to calculate  $\beta$  crystalline phase content ( $F(\beta)$ ) for undrawn PVDF is 44 %, according to Eq.(1). A transformation mechanism of  $\alpha$  to  $\beta$  crystalline phase was reported as the necking region commences. Necking signs the transformation from spherulitic structure to a micro fibrillar one. This mechanism induces all-trans planar zigzag conformation ( $\beta$  crystalline phase) into the crystals [Mohammadi, B., *et al.* 2007]. The calculated  $F(\beta)$  of solution-crystallized and drawn PVDF with different draw ratio are summarized in Table 4.1. The  $F(\beta)$  increases as the draw ratio increase. For DMF solution-crystallized PVDF, high value of  $F(\beta)$  is observed.

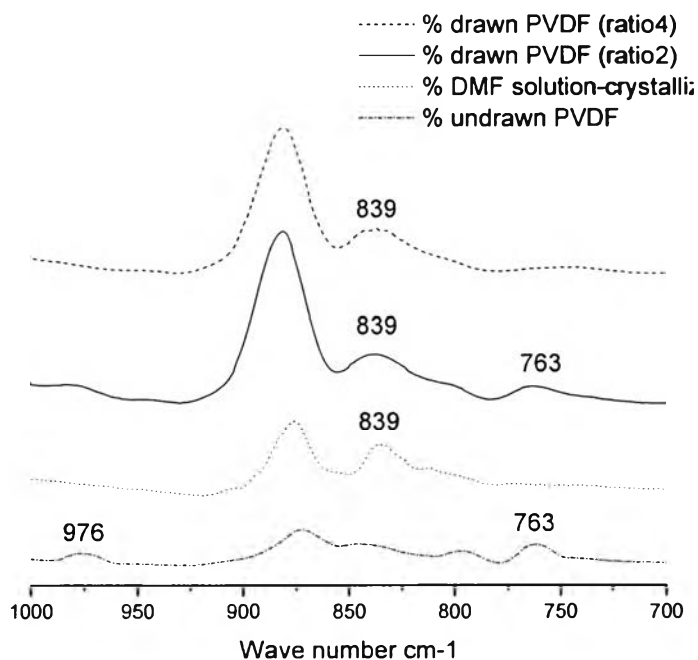


**Figure 4.1** FTIR spectra of undrawn PVDF, DMF solution-crystallized PVDF and drawn PVDF in the different draw ratio from 2 to 4.

**Table 4.1** The variations of  $F(\beta)$  of solution-crystallized PVDF and drawn PVDF with increasing draw ratio at constant drawn rate of 5 min/mm

| Material                       | $\beta$ -phase content, $F(\beta)$ (%) |
|--------------------------------|----------------------------------------|
| undrawn PVDF                   | 44.0                                   |
| DMF solution-crystallized PVDF | 60.4                                   |
| drawn PVDF(ratio2)             | 55.2                                   |
| drawn PVDF(ratio4)             | 59.4                                   |

#### 4.4.2 Scanning electron microscopes-SEM

SEM micrographs of two different fabricated PVDF films are shown in Fig 4.2. Films from solution casting expressed voids generated from solvent evaporate and led to defect on the surface of film. However, compressed film showed smooth

microstructure representing strong film. From these results, PVDF film from compression process is practical to be employed in this research.

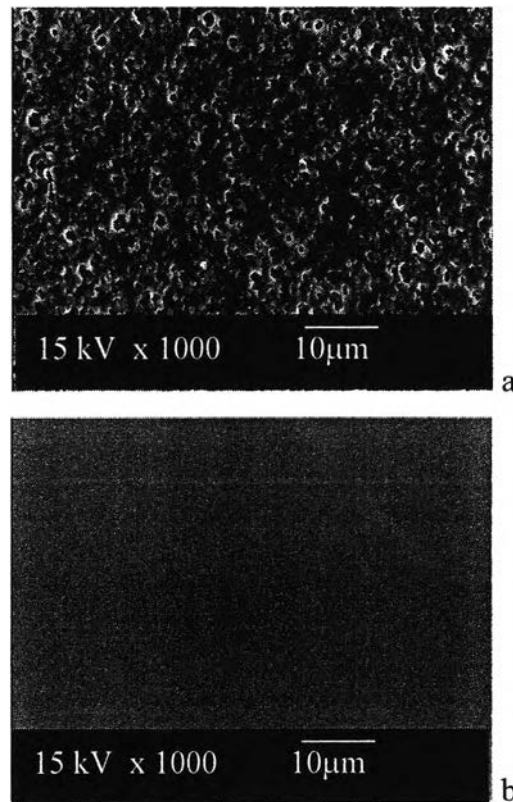


**Figure 4.2** SEM micrographs (a) of solution-crystallized PVDF (b) of compressed PVDF at 174 ° C.

#### 4.4.3 X-ray diffraction (XRD)

XRD measurement was performed to identify the crystal phase of PVDF films. Fig. 4.3 shows the x-ray diffraction patterns of undrawn and drawn PVDF film. From XRD patterns of undrawn PVDF the peaks in  $2\theta$  Bragg angle with values of 20, 27 and 40 corresponding to the plane [(1 1 0),(0 2 1),(0 0 2)] was observed according to Campos[Campos, J. S. C., *et al.* 2007] .These peaks correspond to  $\alpha$  crystalline phase of the PVDF. After the samples were drawn under force, we can find the overlapping of (1 1 1) and (2 0 1) due to the  $\beta$ -phase increases, while the over-

lapping of (1 1 1) and (0 2 1) to 27 theta azimuthally angle reflections of  $\alpha$ -phase disappear according to Ye [Ye, Y., 2004].

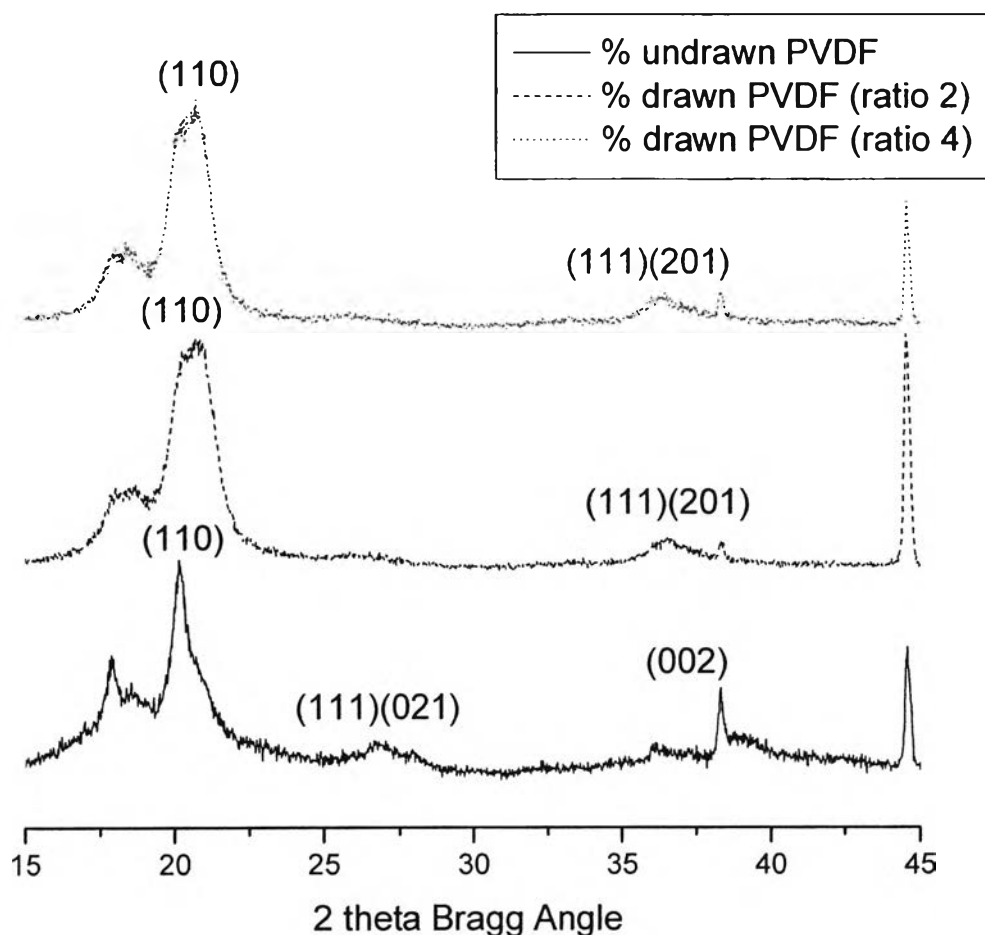


**Figure 4.3** X-ray diffraction patterns of undrawn and drawn of PVDF film.

#### 4.4.4 Dielectric Properties

The variations in the dielectric constant and dielectric loss with frequency for the PVDF are shown in Fig. 4.4 and Fig 4.5 respectively. The dielectric constants of drawn PVDF film are higher than those of undrawn PVDF. The main reason is generated from the existing of  $\beta$  crystalline phase in drawn PVDF film. The dielectric losses of all PVDF films are lower than 0.2 at frequency up to 1 MHz.



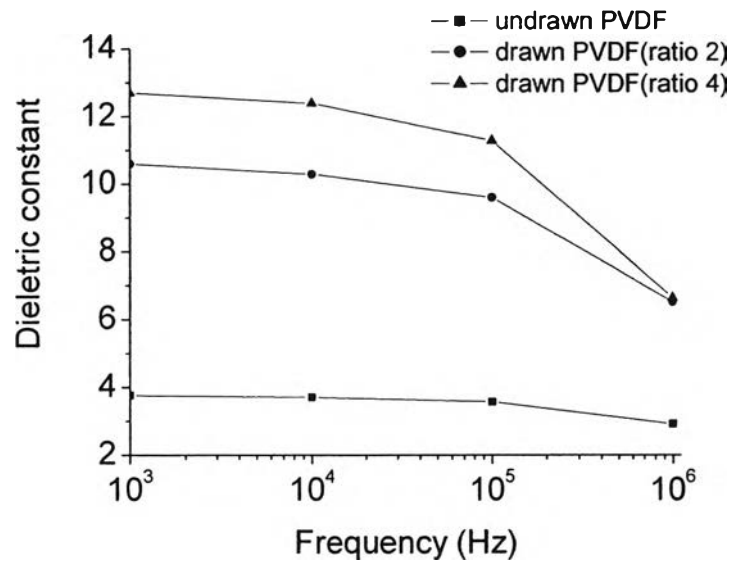


**Figure 4.4** The frequency dependence of the dielectric constant of undrawn and drawn PVDF with ratio 2 and ratio 4

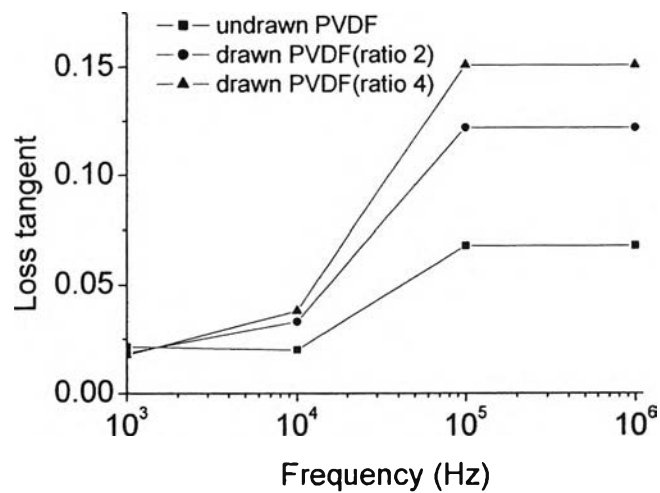


**Figure 4.5** The frequency dependence of the dielectric loss tangent of undrawn and drawn PVDF with ratio 2 and ratio 4.

The variations in dielectric constant and loss tangent with temperature for undrawn PVDF at different frequency are shown in Fig 4.6 and Fig 4.7 respectively. The dielectric constant does not remain constant with temperature because undrawn PVDF shows relaxation process as slipping of molecule PVDF while increasing temperature. The loss tangent of PVDF is lower than 0.4 at all temperature and frequencies.

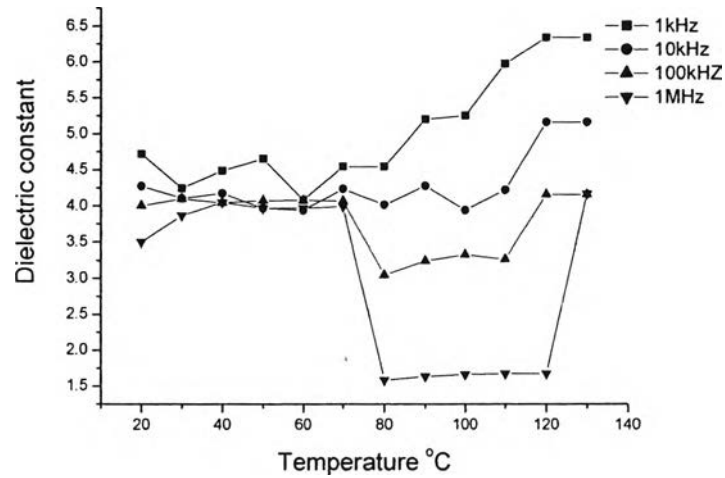


**Figure 4.6** The temperature dependence of dielectric constant for undrawn PVDF at different frequencies.

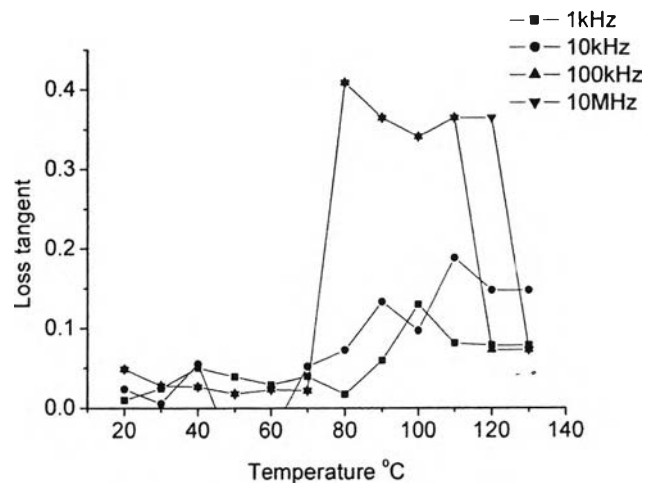


**Figure 4.7** The temperature dependence of loss tangent for undrawn PVDF at different frequencies.

#### 4.4.5 Piezoelectric Properties

The ferroelectric behavior of the undrawn and drawn PVDF are investigated from relationship between polarization ( $P$ ) and electric field ( $E$ ) at room temperature, as shown in Fig. 4.8. The ferroelectric properties are obviously exhibited in drawn PVDF at ratio 2 and 4 which confirm that  $\beta$  crystalline phase is ferroelectric more than  $\alpha$  crystalline phase. From this reasons, the  $\beta$  phase is suitable phase for

ferroelectric application. As seen in the Table 4.2, there is a great difference in stress piezoelectric coefficient ( $d_{33}$ ) of the polarized films before and after stretching. Although the formation of  $\beta$  crystalline phase (with the highest remanant polarization in unit cell) is of main importance in piezoelectric applications, it does not significantly affect the piezoelectric coefficient. Although the mechanical deformation itself induces some preferred crystallite orientations, it does not affect considerably the orientation of molecule dipoles [Mohammadi, B., *et al.* (2007)]. Therefore both undrawn and drawn of PVDF show a zero piezoelectric coefficient. After poling under a constant electric field of 100 kV/mm, at 90°C, the undrawn and drawn PVDF show value of piezoelectric coefficient. It was found that the piezoelectric coefficient of undrawn and drawn PVDF under the same poling conditions increase with an increasing of fraction of  $\beta$  crystalline phase. The highest piezoelectric coefficient for particular poling conditions is reached when the mechanical deformation provides PVDF with the highest content of the polar  $\beta$  crystalline phase along with the high orientation.

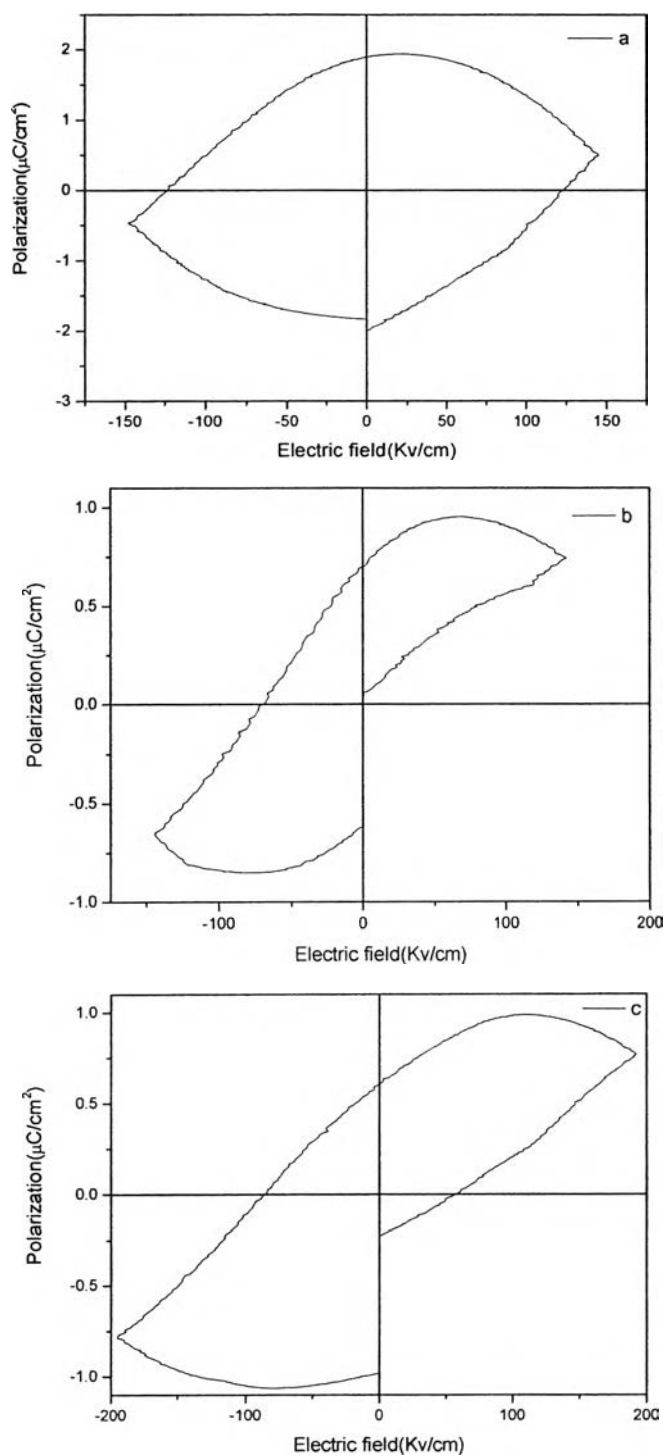


**Figure 4.8** Hysteresis loop of (a) undrawn PVDF (b) drawn PVDF with ratio 2 (c) drawn PVDF with ratio 4.

**Table 4.2** Comparative data of  $d_{33}$  between before and after poling for PVDF film

| Materials             | Piezoelectric coefficient( $d_{33}$ ) |              |
|-----------------------|---------------------------------------|--------------|
|                       | Before poling                         | After poling |
| undrawn PVDF          | 0                                     | 2            |
| drawn PVDF(ratio 2)   | 0                                     | 3            |
| drawn PVDF( ratio 4 ) | 0                                     | 6            |

\*All film were exposed under constant electric field of 100 kV/mm and constant temperature of 90°C

#### 4.4.6 Thermal properties

Figure 4.9 shows the graph of heat flow versus temperature for PVDF at different drawn ratio. It is observed that undrawn and drawn PVDF show endothermic melting peak around 170° C i.e. stretching film does not influence with melting point of films although it increases orientation of molecule. Figure 4.10 shows changes in crystallinity with draw ratio PVDF film. The crystallinity of PVDF increases with draw ratio increases. Crystallinity of the undrawn PVDF is 35% and it abruptly increases up to 44.04% at draw ratio 2 and it increases up to 44.77% at draw ratio 4. This can explain from the fact that drawn PVDF has higher orientation than undrawn PVDF.

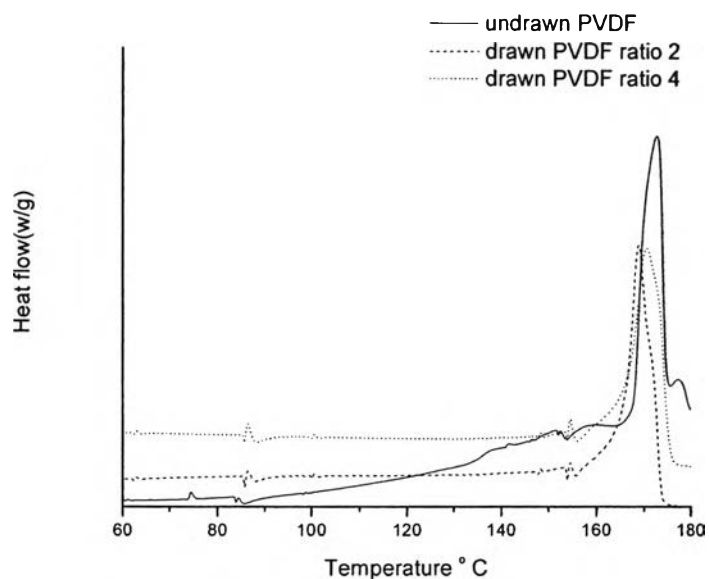


**Figure 4.9** DSC thermograms of undrawn and drawn PVDF.

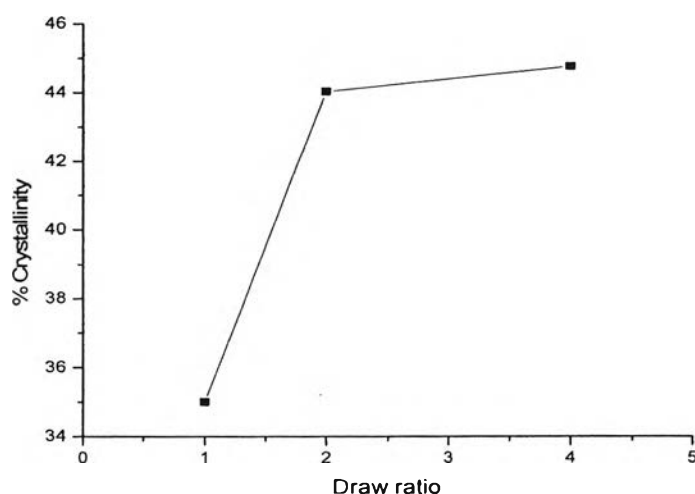


**Figure 4.10** Percent total crystallinity versus draw ratio of PVDF.

## 4.5 Conclusions

The  $\beta$  crystalline phase of PVDF films have been investigated by technique of Fourier Transform Infrared Spectroscopy (FTIR). It can be calculated that F ( $\beta$ ) value is high in DMF solution-crystallized PVDF and high draw ratio which corresponding to piezoelectric properties, However, SEM micrographs show defect of PVDF film fabricated from solution casting therefore compressed PVDF was selected. Increasing of  $\beta$  crystalline phase can be confirmed by XRD diffraction as the

draw ratio increase. The piezoelectric properties are investigated resulting the increasing of dielectric constant with increasing drawn ratio. The ferroelectric properties are observed in high  $\beta$  crystalline PVDF films. It can be concluded that the ferroelectric properties are governed by  $\beta$  phase. The piezoelectric coefficient of undrawn and drawn PVDF under the same poling conditions increases with an increasing fraction of  $\beta$  crystalline phase. The stretching PVDF film has no effect on melting temperature but has effect on crystallinity of PVDF film.

#### 4.6 Acknowledge

The authors wish to thank MTEC staffs for useful assistance and instrument for characterizations. The partial funding of research work was provided by PPT consortium and Polymer Processing and Nanomaterials research unit.

#### 4.7 References

- Campos, J. S. C., Ribeiro, A. A. and X.Cardoso, C. (2007) Preparation of characterization of PVDF/CaCO<sub>3</sub> composites, Journal of Materials Science & Engineering B, 136, pp 123-128.
- Kim, B. S., Lee, J.Y. and PorTer, R.S.(1998) The Crystalline phase Transformation of Poly(Vinylidene Fluoride)/Poly(vinyl Fluoride) Blend Films, Polymer Engineering And Science, 38(9), pp 1359-1365.
- Mohammadi, B., Yousefi, A.A, Bellah, S. M. (2007) Effect of tensile strain rate and elongation on crystalline structure and piezoelectric properties of PVDF thin films, Polymer Testing, 26, pp 42-50.
- Rollik, D., Bauer, S. and Gerhard-Multhaupt, R. (1999) Separate contributions to the pyroelectricity in poly(vinylidene fluoride) from the amorphous and crystalline phases, as well as from their interface, Journal of Applied Physics, 85(6), pp 3282-3288.

- Salimi, A., Yousefi, A.A. (2004), Conformational changes and phase transformation mechanisms in PVDF solution-cast films, Journal of Polymer Science: Part B: Polymer Physics, 42, pp 3487–3495
- Salimi, A., Yousefi, A.A. (2003) FTIR studies of b-phase crystal formation in stretched PVDF films, Polymer Testing, 22, pp 699.
- Ye, Y., Jiang, Z., Wu, Y., Zwng, H., Yang, Y. and Li W (2004) Characterization and Ferroelectric Properties of Electric Poled PVDF Films, School of optoelectronic Information, University of Electric Science and Technology of China.